A TP63 Mutation Causes Prominent Alopecia with Mild Ectodermal Dysplasia

Sabine Duchatelet, Claudia Russo, Christian Osterburg, Stéphanie Mallet,
Christine Bole-Feysot, Patrick Nitschke, Marie-Aleth Richard, Volker Dötsch,
Caterina Missero, Aude Nassif, et al.

A *TP63* Mutation Causes Prominent Alopecia with Mild Ectodermal Dysplasia

TO THE EDITOR

TP63 mutations are the primary source of several autosomal dominant ectodermal dysplasias, which are characterized by various combinations of limb, ectodermal, and orofacial abnormalities (Rinne et al., 2007). We describe a family with prominent alopecia and mild ectodermal dysplasias features, which co-segregate with a *TP63* mutation.

The institutional review board of CPP Ile-de-France, Paris, approved this study. Subjects or parents provided written informed consent to participate in this study along with the consent to publish their images.

An autosomal dominant inheritance pattern was observed in the studied family, which belonged to the Algerian ancestry (Figure 1). All patients had coarse and uncombable hair since birth, later persisting into adulthood. Alopecia was developed around 25 years of age, first starting in the parieto-temporal areas and further progressing to almost complete non-scarring hair loss in men after 50 years of age or it was restricted to the parieto-temporal areas in female patient IV.5 that was clinically similar to alopecia areata (Figure 1). In addition, body hair was sparse or absent along with scanty eyebrows and eyelashes. A careful examination revealed additional subtle ectodermal abnormalities (onychodystrophia of the first toe, ichthyosis, and hypohidrosis), lacrimal duct atresia, and photophobia (Figure 1). Patient IV.5 had oral and palate cleft at birth. Patient IV.8 had bifidal uvula and severe keratitis. All patients had yellow teeth without an early loss or abnormal shape. Other anomalies included unexplored gynecomastia (III.8) and vaginal synechiae (IV.5). Altogether, these minor ectodermal abnormalities suggested an unclassified form of ectodermal dysplasias.

We performed a linkage study by using single nucleotide polymorphisms and whole-exome sequencing in five members of a family (Figure 1). The linkage study analysis revealed no genomic locus with a significant signal. The maximum value of linkage (logarithm of odds score = 0.6021) was observed in 25 genomic regions (Supplementary Table S1). Variants identified by whole-exome sequencing were selected based on an autosomal dominant model, which was caused by a rare heterozygous mutation. Variants present in the databases or previously observed in the in-house exomes with a minor allele frequency > 1were excluded. Heterozygous coding or splicing variants that were predicted to be damaging by the in silico prediction tools were selected, thereby leading to an identification of nine variants segregating with the disease and located within one of the regions with a logarithm of odds score of 0.6021 (Supplementary Table S2). Eight of these variants were confirmed by Sanger sequencing, and these were subsequently sequenced in nine additional family members. Only one variant was segregated with the disease. In contrast to unaffected individuals, all patients were heterozygous for the c.574T > C variant (NM_003722) within the *TP63* gene leading to p.Trp192Arg (NP_003713). This variant had not been previously reported and involved a highly conserved residue among species.

TP63 encodes the transcription factor p63, which is a key regulator of ectodermal, orofacial, and limb development (Rinne et al., 2007). The use of different transcription initiation sites and alternative splicing generates several *TP63* isoforms (ΔN or TA and α, β, γ, δ, or ε, respectively).

TP63 mutations cause ectrodactyly, ectodermal dysplasia, and cleft lip/palate syndrome (EEC); acro-dermato-ungual-lacrimal-tooth syndrome (ADULT); ankyloblepharon-ectodermal defects-cleft lip/palate (AEC); Rapp−Hodgkin and limb mammary syndromes; isolated split hand/foot malformation 4; and non-syndromic cleft lip (Supplementary Table S3) (Rinne et al., 2007). The p.Trp192Arg mutation is localized in the p63 DNA-binding domain (DBD) (Supplementary Figures S1 and S2) (Enthart et al., 2016). This residue, buried in the protein structure, is not known for being a key residue for DNA binding (Supplementary Figure S2); however, it is predicted to result in protein instability and malfunction by computational tools (Supplementary Table S4). This residue introduces an uncompensated positive charge and cause the loss of interaction mediated by the Trp side chain. It is expected to cause steric clashes in every possible side chain conformation, thereby assuming that the overall structure does not change (Supplementary Figure S2). Hence, the local structure is predicted to be disrupted and affect the p63 function. To assess the consequences of the p.Trp192Arg mutation, wild-type or mutant proteins, containing either the p.Trp192Arg or the previously reported p.Arg343Gln EEC and p.Leu553Phe AEC mutations, localized in the DBD and the sterile-α-motif domain, respectively, were assayed for their ability to transactivate a reporter gene under the control of the *KRT14* promoter gene. In contrast to the wild-type ΔNp63α, which showed a potent transactivation, EEC and AEC mutants failed to drive the expression of the reporter gene as previously reported (Figure 2). Conversely, the

---

ARTICLE IN PRESS

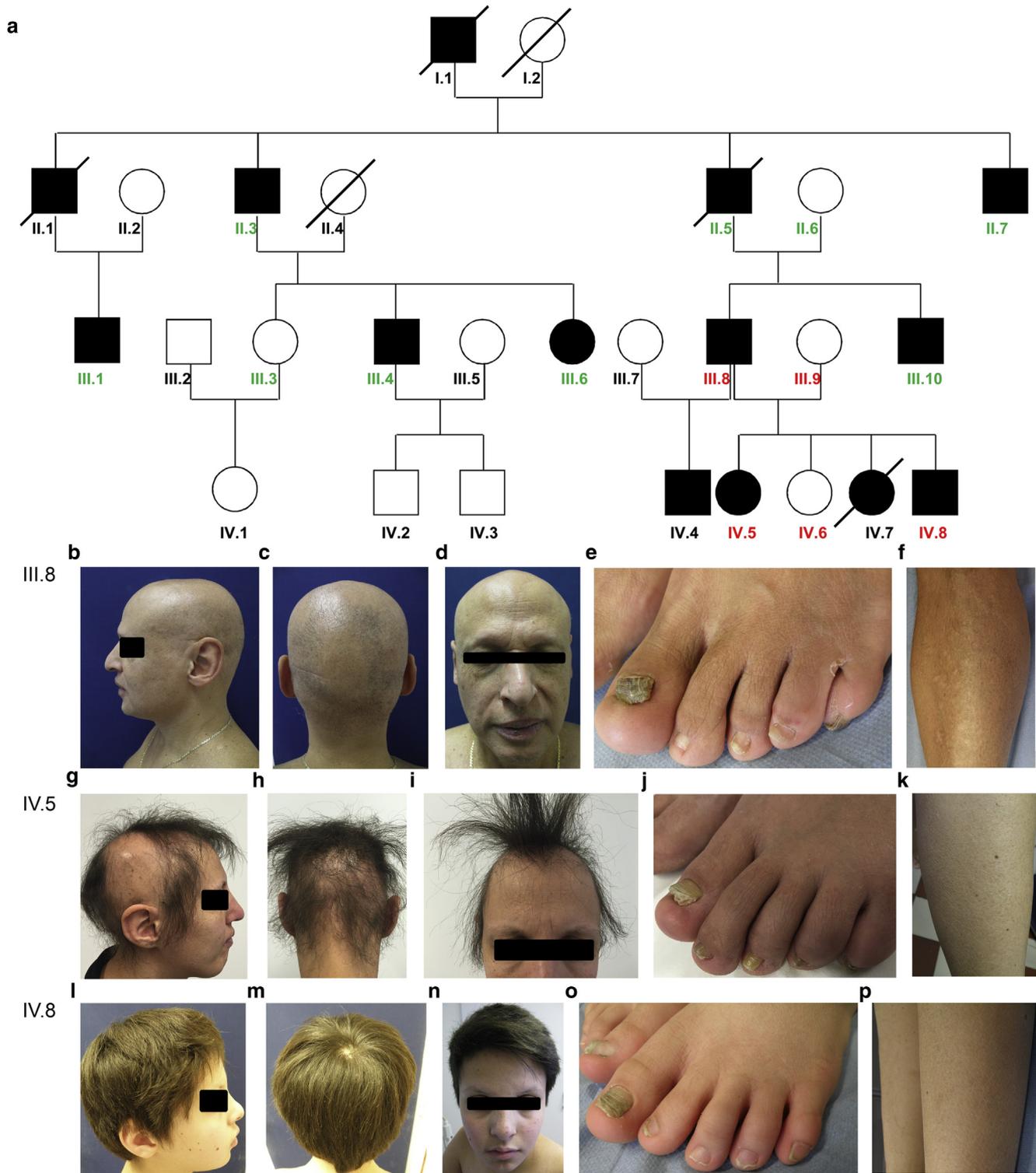*S Duchatelet* et al.
Alopecia by *TP63* mutation

Figure 1. Family pedigree and clinical features. (**a**) Family pedigree. This family comprises 14 affected and 13 unaffected individuals. The first individuals who were studied by exome sequencing are indicated in red, whereas the individuals who were subsequently studied are indicated in green. Patient IV.7 who died from sudden infant death had coarse hair, further suggesting that she was also affected. (**b**–**p**) Clinical features. Clinical presentation of patients (**b**–**f**) III.8 at 63 years, (**g**–**k**) IV.5 at 41 years, and (**l**–**p**) IV.8 at 13 years. (**b**–**d**), (**g**–**i**), and (**l**–**n**) Hair abnormalities, and (**b**–**d**) and (**g**–**i**) hair loss, abnormal toe nails are restricted (**e** and **o**) to the first toe or (**j**) it involves all toes and (**f**, **k**, and **p**)dry skin with mild ichthyosis. Of note, patient IV.8 has not yet developed alopecia because of his age. Subjects or parents consented to the publication of their images.

p.Trp192Arg mutant presented with a slightly increased transactivation activity than the wild-type (Figure 2). Similar results were obtained with ΔNp63γ and TAp63α isoforms. In contrast, the p.Trp192Arg mutant displayed a decreased transactivation activity on the ΔNp63β isoform, and no effect was observed on TAp63β and TAp63γ isoforms. Other *TP63* mutations are known to increase isoform-specific, promoter-dependent
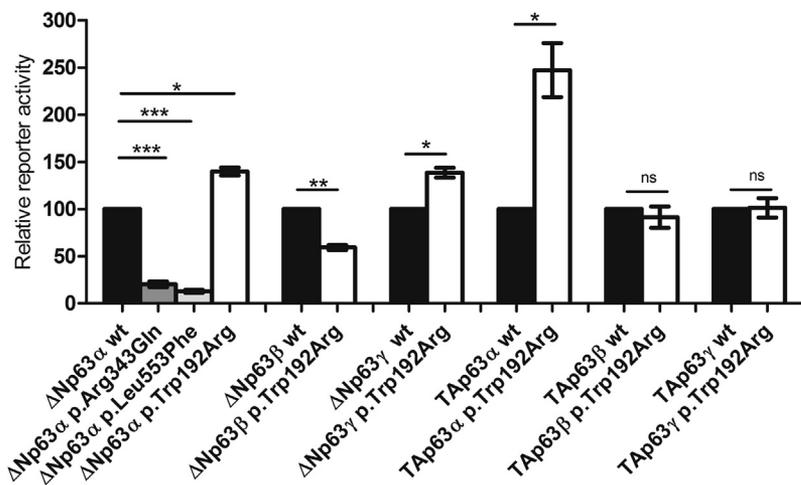
Figure 2. Effects of *TP63* mutations on the transactivation activity of the Keratin 14 promoter. The mutant transactivation activity is indicated as the percentage of the corresponding wt counterpart isoform. Reported assay demonstrated that the p.Trp192Arg *TP63* mutant has an increased transactivation activity on ΔNp63α, ΔNp63γ, and TAp63α isoforms, a decreased transactivation activity on ΔNp63β, and no effect on TAp63β and TAp63γ isoforms. ns, not significant; wt, wild-type. $*P < 0.05$; $**P < 0.01$; $***P < 0.001$.

transcriptional activity (Browne et al., 2011; Duijf et al., 2002).

The main symptoms generally observed in the *TP63*-associated syndromes are summarized in Supplementary Table S3 (Brunner et al., 2002; Rinne et al., 2007, 2006a). Our cases lack the main clinical features of these syndromes (ankyloblepharon at birth for AEC, limb defects and excessive freckling in the sun-exposed areas for ADULT). However, a large clinical variability and frequent overlap between these syndromes are observed, and these features are inconstant and not fully specific (van Straten and Butow, 2013). Of note, three atypical cases with *TP63* mutations presenting with a phenotype not clearly related to any *TP63*-associated syndromes have previously been reported (Goldsmith et al., 2014; Kawai et al., 2018; Ruml et al., 2015).

EEC syndrome mutations mainly cluster in the DBD, thus disturbing the p63-DNA binding and leading to the loss of transactivation, whereas the AEC syndrome mutations are mainly located in the sterile-α-motif and transactivation inhibitory domains, thereby leading to unfolding and p63 aggregation (Rinne et al., 2006a; Russo et al., 2018). However, some DBD mutations were also identified in patients with ADULT or AEC syndrome, limb mammary syndrome, non-syndromic cleft lip, and split hand/foot malformation (Supplementary Figure S1). In contrast to the EEC-associated mutations, DBD ADULT-mutations are located at a distance from the p63—DNA interaction surface and confer a gain of transactivation activity (Duijf et al., 2002; Rinne et al., 2006b). Thus, differences in clinical manifestations associated with EEC, ADULT, or p.Trp192Arg DBD mutations might result from the distinct effects of these mutant proteins on the transactivation of p63 target genes. The p.Trp192Arg mutation could predominantly affect the transactivation of p63 target genes previously involved in hair follicle growth, thus explaining the observed phenotype with prominent alopecia and minor ectodermal anomalies (Clements et al., 2012; Fiuraskova et al., 2005; Romano et al., 2010).

These findings expand the spectrum of *TP63*-associated clinical manifestations, illustrate the diagnostic complexity of *TP63* phenotypes, and lead to the search for *TP63* mutations in the familial progressive alopecia.

Data availability statement
Exome sequencing datasets related to this article are hosted at the NCBI Sequence Read Archive under the accession code PRJNA550013.

ORCIDs
Sabine Duchatelet: https://orcid.org/0000-0003-2537-0385
Claudia Russo: https://orcid.org/0000-0001-5869-4445
Christian Osterburg: https://orcid.org/0000-0002-2144-583X
Stéphanie Mallet: https://orcid.org/0000-0003-2884-0645
Christine Bole-Feysot: https://orcid.org/0000-0002-1935-3063
Patrick Nitschké: https://orcid.org/0000-0002-2094-3298
Marie-Aleth Richard: https://orcid.org/0000-0002-0870-9132
Volker Dötsch: https://orcid.org/0000-0001-5720-212X
Caterina Missero: https://orcid.org/0000-0003-0905-5123
Aude Nassif: https://orcid.org/0000-0002-2407-0834
Alain Hovnanian: https://orcid.org/0000-0003-3412-7512

CONFLICT OF INTEREST
The authors state no conflict of interest.

Sabine Duchatelet[1,2], Claudia Russo[3], Christian Osterburg[4], Stéphanie Mallet[5], Christine Bole-Feysot[2,6], Patrick Nitschké[2,7], Marie-Aleth Richard[5], Volker Dötsch[4], Caterina Missero[3], Aude Nassif[8] and Alain Hovnanian[1,2,9,*]

[1]Laboratory of Genetic Skin Diseases, INSERM Imagine Institute, Paris, France; [2]Paris Descartes University, Paris, France; [3]CEINGE Biotecnologie Avanzate and Department of Biology, University of Naples Federico II, Naples, Italy; [4]Institute of Biophysical Chemistry and Center for Biomolecular Magnetic Resonance, Goethe University, Frankfurt, Germany; [5]Dermatology Department, EA 3279: CEReSS -Health Service Research and Quality of Life Center, Timone Hospital, Assistance Publique Hôpitaux de Marseille, Aix-Marseille University, Marseille, France; [6]Genomic Platform, INSERM Imagine Institute, Paris, France; [7]Bioinformatics Platform, INSERM Imagine Institute, Paris, France; [8]Medical Center, Institut Pasteur, Paris, France; and [9]Department of Genetics, Necker—Enfants Malades Hospital, Assistance Publique des Hôpitaux de Paris, (AP-HP), Paris, France
*Corresponding author e-mail: alain.hovnanian@inserm.fr

ARTICLE IN PRESS

S Duchatelet et al.
Alopecia by *TP63* mutation

REFERENCES

Browne G, Cipollone R, Lena AM, Serra V, Zhou H, van Bokhoven H, et al. Differential altered stability and transcriptional activity of ΔNp63 mutants in distinct ectodermal dysplasias. J Cell Sci 2011;124:2200−7.

Brunner HG, Hamel BC, Van Bokhoven H. The p63 gene in EEC and other syndromes. J Med Genet 2002;39:377−81.

Clements SE, Techanukul T, Lai-Cheong JE, Mee JB, South AP, Pourreyron C, et al. Mutations in AEC syndrome skin reveal a role for p63 in basement membrane adhesion, skin barrier integrity and hair follicle biology. Br J Dermatol 2012;167:134−44.

Duijf PH, Vanmolkot KR, Propping P, Friedl W, Krieger E, McKeon F, et al. Gain-of-function mutation in ADULT syndrome reveals the presence of a second transactivation domain in p63. Hum Mol Genet 2002;11:799−804.

Enthart A, Klein C, Dehner A, Coles M, Gemmecker G, Kessler H, et al. Solution structure and binding specificity of the p63 DNA binding domain. Sci Rep 2016;6:26707.

Fiuraskova M, Brychtova S, Kolar Z, Kucerova R, Bienova M. Expression of beta-catenin, p63 and CD34 in hair follicles during the course of androgenetic alopecia. Arch Dermatol Res 2005;297:143−6.

Goldsmith T, Eytan O, Magal L, Solomon M, Israeli S, Warshauer E, et al. A mutation in TP63 causing a mild ectodermal dysplasia phenotype. J Invest Dermatol 2014;134:2277−80.

Kawai T, Hayashi R, Nakai H, Shimomura Y, Kurban M, Hamie L, et al. A heterozygous mutation in the SAM domain of p63 underlies a mild form of ectodermal dysplasia. J Dermatol Sci 2018;90:360−3.

Rinne T, Brunner HG, van Bokhoven H. p63-associated disorders. Cell Cycle 2007;6:262−8.

Rinne T, Hamel B, van Bokhoven H, Brunner HG. Pattern of p63 mutations and their phenotypes–update. Am J Med Genet A 2006a;140:1396−406.

Rinne T, Spadoni E, Kjaer KW, Danesino C, Larizza D, Kock M, et al. Delineation of the ADULT syndrome phenotype due to arginine 298 mutations of the p63 gene. Eur J Hum Genet 2006b;14:904−10.

Romano RA, Smalley K, Liu S, Sinha S. Abnormal hair follicle development and altered cell fate of follicular keratinocytes in transgenic mice expressing DeltaNp63alpha. Development 2010;137:1431−9.

Ruml J, Cuturilo G, Lukac M, Peters H. Ectodermal defects and anal atresia in a child with a TP63 mutation–expanding the phenotypic spectrum. Pediatr Dermatol 2015;32:421−2.

Russo C, Osterburg C, Sirico A, Antonini D, Ambrosio R, Würz JM, et al. Protein aggregation of the p63 transcription factor underlies severe skin fragility in AEC syndrome. Proc Natl Acad Sci USA 2018;115:E906−15.

van Straten C, Butow KW. Gene p63: in ectrodactyly-ectodermal dysplasia clefting, ankyloblepharon-ectodermal dysplasia, Rapp-Hodgkin syndrome. Ann Maxillofac Surg 2013;3:58−61.

ARTICLE IN PRESS

S Duchatelet et al.
Alopecia by *TP63* mutation

SUPPLEMENTARY MATERIALS AND METHODS

Genomic DNA

Genomic DNA was isolated from peripheral blood by using a standard phenol chloroform protocol. DNA purification was performed by using Amicon Ultra 30K centrifugal filter units (Millipore, Burlington, MA).

Linkage study

The five members from the initial nuclear family were genotyped with the Affymetrix Human Mapping 250K Nsp Array (262,000 single nucleotide polymorphisms, Thermo Fischer, Waltham, MA). All genotyping procedures were performed as per the manufacturer's protocols. The logarithm of odds scores were calculated by using the program MERLIN software (version 1.1.2) based on a standard disease model for rare dominant conditions with complete penetrance.

Exome sequencing and mutation confirmation

Bar-coded DNA libraries were prepared, and the exome capture (Agilent 50 Mb SureSelect Human All Exon V3, Santa Clara, CA) and sequencing (Life Technologies SOLiD5500, Thermo Fischer) was performed. Resulting reads (75 base pairs) were generated with the Exact Call Chemistry and aligned to the human reference sequence (hg19) with LifeScope (Life Technologies), and variants were called with GATK (Broad Institute, Cambridge, MA) and annotated with the in-house software (Poly-Web; Imagine Institute, Paris, France). The mean coverage was x50−60, with 80−82% of bases covered $\geq$ x15. Of note, no mutations in U2HR or EPS8L3 genes responsible for the Marie−Unna hereditary hypotrichosis (OMIM 146550) were identified in these patients. For variant filtering, the databases, dbSNP, 1000 Genomes, and Exome Sequencing Project, and the in

silico prediction tools, SIFT and PolyPhen-2, were used. We sequenced the nine whole-exome sequencing candidate variations in the initial five individuals by using Sanger sequencing with the standard protocols (Applied Biosystems 3130xl, Thermo Fischer). The eight variants, which were confirmed by Sanger sequencing, were subsequently sequenced in the additionally recruited family members. Only one variant segregated with the trait in all family members was studied. Additional prediction tools were used to predict the pathogenicity of this variant identified by exome sequencing:

1. Panther (http://www.pantherdb.org/)
2. LRT (http://www.genetics.wustl.edu/jflab/lrt_query.html)
3. MutationTaster (http://www.mutationtaster.org/)
4. MutationAssessor (http://mutationassessor.org/r3/)
5. AlignGVGD (http://agvgd.hci.utah.edu/agvgd_input.php)
6. SNAP2 (https://www.rostlab.org/services/SNAP/)
7. SNP&GO (https://snps-and-go.biocomp.unibo.it/snps-and-go/)
8. Condel (http://bbglab.irbbarcelona.org/fannsdb/signin?next=%2Ffannsdb%2Fquery%2Fcondel)
9. FATHMM (http://fathmm.biocompute.org.uk/fathmm-xf/)
10. MutPred (http://mutpred.mutdb.org/#qform)

Protein stability change prediction tools

The computational tools indicated below were used to predict the protein stability change resulting from the mutation p.Trp192Arg:

1. SAAFEC (http://compbio.clemson.edu/SAAFEC/userInputParams.html)
2. SDM (http://marid.bioc.cam.ac.uk/sdm2/prediction)

3. mCSM (http://biosig.unimelb.edu.au/mcsm/stability)
4. MAESTRO (https://biwww.che.sbg.ac.at/maestro/web/maestro/)
5. I-Mutant (http://folding.biofold.org/i-mutant/i-mutant2.0.html)
6. PoPMuSiC (https://soft.dezyme.com/query/create/pop)
7. DUET (http://biosig.unimelb.edu.au/duet/stability/)
8. iStable (http://predictor.nchu.edu.tw/iStable/)

Transactivation study

Wild-type ΔNp63α, ΔNp63β, ΔNp63γ, TAp63α, TAp63β, and TAp63γ isoforms were cloned into the pcDNA3_C-Myc expression vector. We then introduced the c.574T > C variant (NM_003722) into the p63 construct by using the Q5 Site-Directed Mutagenesis Kit (New England Biolabs, Ipswich, MA). The wild-type p63 or the mutant p63 construct were co-transfected into the HEK293T together with a plasmid carrying the promoter of the Keratin 14 gene, which is a target of *TP63*, located upstream to the luciferase gene and with renilla luciferase. The luciferase activity was measured 48 hours after transfection. The experiment was replicated four times. The mutant transactivation activity was indicated as the percentage of the respective wild-type counterpart.

### Statistics

Statistical significance of observed differences was assessed by the two-tailed t-test. Means with standard error of mean are shown.

SUPPLEMENTARY REFERENCE

Klein C, Georges G, Künkele KP, Huber R, Engh RA, Hansen S. High thermostability and lack of cooperative DNA binding distinguish the p63 core domain from the homologous tumor suppressor p53. J Biol Chem 2001;276:37390−401.

ARTICLE IN PRESS

S Duchatelet et al.
Alopecia by *TP63* mutation
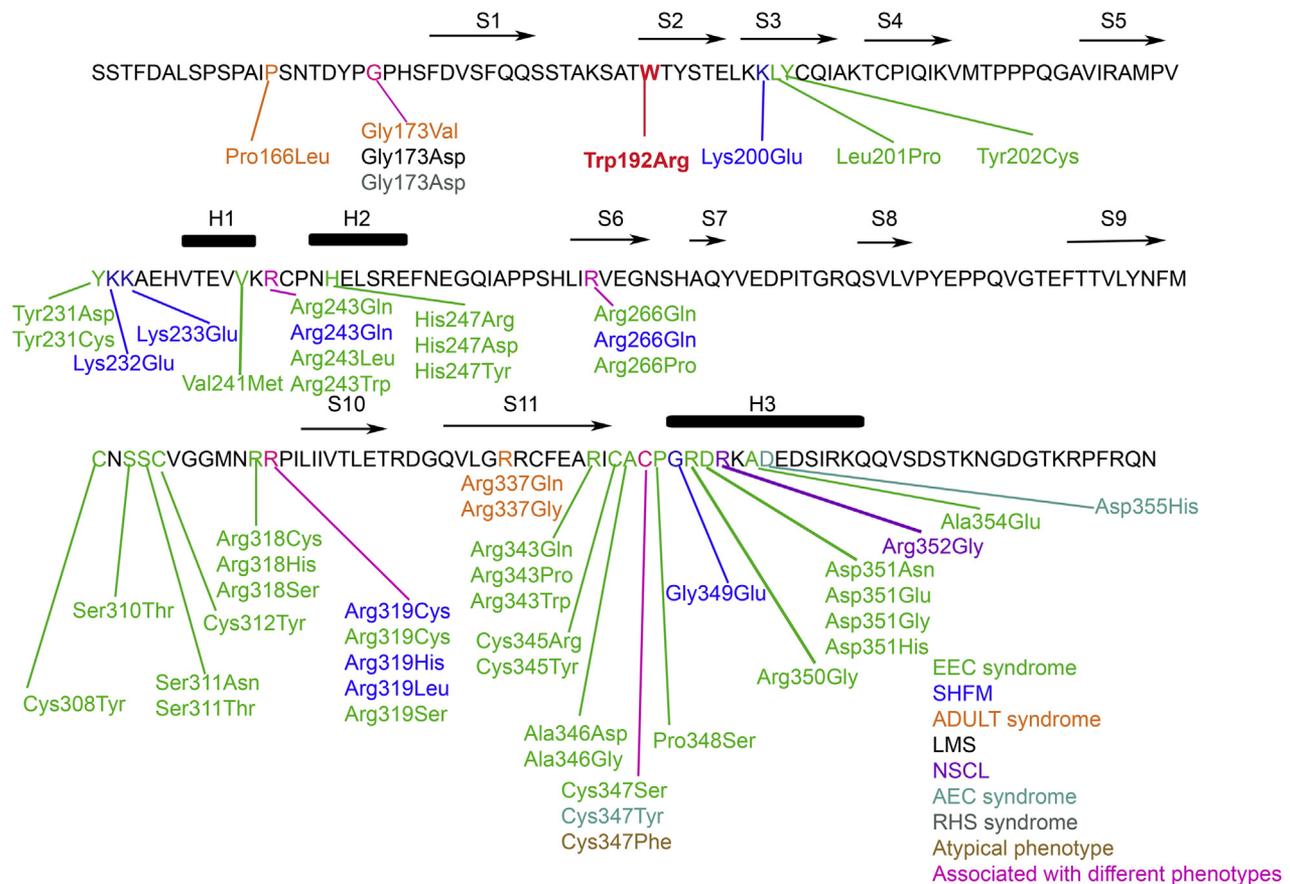
Supplementary Figure S1. Sequence of *TP63* DBD with reported missense mutations and associated phenotypes. α-helixes are indicated by black boxes (H1—H3), and β-strands by arrows (S1—S11) (Protein Data Bank PDB 2RMN). Reported missense mutations within the DBD and the associated phenotypes are coded with color. The mutation p.Trp192Arg identified in this report is indicated in red. Other reported DBD mutations included splicing mutations c.580-2A>G (EEC) and c.580-2A>C (SHFM), a small deletion mutation p.Ile324del (EEC) and a frameshift mutation p.Gln274Profs*4 (NSCL). ADULT, acro-dermato-ungual-lacrimal-tooth syndrome; AEC, ankyloblepharon-ectodermal defects-cleft lip/palate; DBD, DNA-binding domain; EEC, ectrodactyly, ectodermal dysplasia, and cleft lip/palate syndrome; LMS, limb mammary syndrome; NSCL, non-syndromic cleft lip; RHS, Rapp—Hodgkin syndrome; SHFM, split hand/foot malformation.
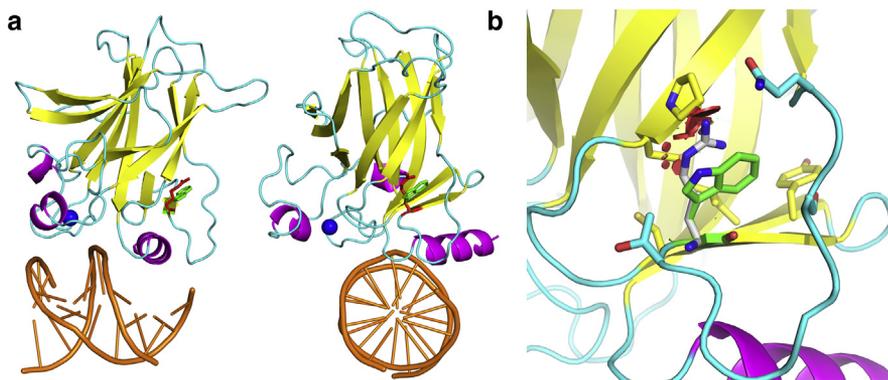
Supplementary Figure S2. DBD structure and Trp192Arg *TP63* mutation. (**a**) Two different views of the DBD structure with the localization of residue 192. α-helixes are indicated in purple, β-strands in yellow, and DNA in orange. DBD is composed of 3 α-helixes and 11 β-strands. Trp192 is a buried residue localized in the S2 β-strand. Trp is represented in green and Arg in red. The Trp192Arg nonconservative missense mutation predominantly changes the chemistry (non-polar and aromatic amino acid vs. charged aliphatic residue) of residue 192 and is predicted to alter the protein stability (Supplementary Table S2). (**b**) Magnified image of the position of residue 192. Substitution of Trp192 (in green), for Arg (in gray), which are superposed on the figure, causes steric clashes (red plates) in every possible side chain conformation (one representative rotamer shown), introduces an uncompensated positive charge and results in the loss of interactions mediated by the Trp side chain, thereby suggesting the disruption of the local structure, which secondarily affects the DNA binding interface of the DBD. PDB file 3QYM generated the images. DBD, DNA-binding domain; PDB, Protein data bank.

ARTICLE IN PRESS

S Duchatelet et al.
Alopecia by *TP63* mutation

Supplementary Table S1. Linkage Study Data

Chromosome	Start	End	size in Mb
1	22629057	43299121	20.67
	224888632	237997087	13.10
2	681521	19798230	19.12
	19911287	42762739	22.85
	239733773	242920779	3.26
3	141623372	190273818	48.65
4	79719	2087049	2.01
	102172981	124522628	22.35
5	76371119	158022041	81.65
6	6667169	25676397	19.01
	25697576	50596286	24.90
	163122220	168965542	5.84
7	7294802	82473388	75.18
	104177313	147710188	43.53
8	111112499	146195832	35.18
11	440343	16459560	16.09
	81236034	133392294	52.16
16	988998	2824984	2.17
	79083939	89339571	10.75
17	5960849	37081707	31.12
19	13353722	51332670	37.98
20	1112168	6881898	5.77
	6922676	42357295	35.43
21	14691367	25807198	11.16
22	28165334	45253872	17.09

Regions with a logarithm of odds score of 0.6021 (maximum logarithm of odds score obtained).

Supplementary Table S2. Candidate Heterozygous Variants Segregating with the Disease Identified by Whole-Exome Sequencing After Filtering

Gene	Chromosome	Location	Nucleotide change	Consequence
CAPN14	2	31423319	c.723_724del (NM_001145122)	p.Lys244Aspfs*25
TP63	3	189526310	c.574T>C (NM_003722)	p.Trp192Arg
MAN2A1	5	109103307	c.907C>T (NM_002372)	p.Arg303Cys
PCDHB15	5	140627233	c.2087C>G (NM_018935)	p.Ser696Trp
MLXIPL	7	73009983	c.2294A>G (NM_032951)	p.Asn765Ser
KIAA1147	7	141385278	c.527G>A (NM_001080392)	p.Arg176Gln
ZDHHC7[1]	16	85010049	c.826_827insCT (NM_017740)	p.Gly276Alafs*10
COPRS	17	30183820	c.164T>C (NM_018405)	p.Leu55Pro
ZNF546	19	40521649	c.2472G>C (NM_178544)	p.Gln824His

[1]This variant was not confirmed by Sanger sequencing.

ARTICLE IN PRESS

S Duchatelet et al.
Alopecia by *TP63* mutation

Supplementary Table S3. Clinical Features Observed in p63-Associated Syndromes and Present Cases

Clinical features	EEC	ADULT	AEC	RHS	LMS	Present cases
Limbs malformations	+	+	-	-	+	-
Orofacial clefting	+	-	+	+	+	1/14 case (IV.5)
Skin abnormalities	+	+	+	+	-	all cases
Scalp erosions	-	-	+	-	-	-
Hypohidrosis	-	-	-	+	+	all cases
Abnormal hair	+	+	+	+	-	all cases
Abnormal nails	+	+	+	+	-	all cases
Abnormal teeth	+	+	+	+	-	all cases
Lacrimal puncta defects	+	+	+	+	+	all cases
Photophobia	+	-	+	+	-	all cases
Ankyloblepharon	-	-	+	-	-	-
Mammary gland anomalies	-	+	-	-	+	1/14 case (III.8)
Hearing lost	-	-	+	+	-	-
Freckling	-	+	-	-	-	-
Urogenital abnormalities	+	-	+	+	-	1/14 case (IV.5)

+ indicates that this phenotype is frequently observed in patients with this condition.

- indicates that this feature is never or rarely reported in patients with this syndrome.

Alopecia is sometimes observed; however, eyelashes and eyebrows are occasionally absent in EEC, ADULT, AEC, and RHS syndromes. Teeth anomalies with poor enamel formation and nail abnormalities are frequently observed in EEC, ADULT, AEC, and RHS syndromes. The absence or reduced amount of sweat glands leading to hypohidrosis (mainly in RHS and LMS) and lacrimal duct defects (EEC, ADULT, AEC, RHS, and LMS) are also reported among patients with TP63 mutations. Photophobia can be observed in EEC, RHS, and AEC. Thin and dry skin resembling dermatitis is observed in EEC, ADULT, and RHS syndromes. Skin anomalies are more severe (scalp erosions) in the AEC syndrome. Orofacial clefting is frequently observed in EEC, AEC, RHS, and LMS syndromes but rarely in the ADULT syndrome. NoAnkyloblepharon or minor eyelid abnormalities were not noticed at birth. In addition, no hearing loss, no ectro- or syndactyly, no supernumerary or hypoplastic nipples, and no freckling were observed in the present cases. Of note, patients had normal fingernails and no palmoplantar keratoderma.

Abbreviations: ADULT, acro-dermato-ungual-lacrimal-tooth syndrome (OMIM 103285); AEC, ankyloblepharon-ectodermal defects-cleft lip/palate (OMIM 106260); EEC, ectrodactyly, ectodermal dysplasia, and cleft lip/palate syndrome (OMIM 604292); RHS, Rapp—Hodgkin syndrome (OMIM 129400); LMS, limb mammary syndrome (OMIM 603543).

Supplementary Table S4. Consequence of p.Trp192Arg *TP63* Mutation on Protein Stability

Prediction tools	Stability Change ($\Delta\Delta G$ Kcal/mol)
SDM	-2.02[1]
mCSM	-1.30[1]
SAAFEC	-5.50[1]
i-Mutant	-3.11[1]
DUET	-1.21[1]
iStable	-2.19[2]
PoPMuSiC	2.81[2]
Maestro	2.07[2]

The prediction of the effect of p.Trp192Arg TP63 mutation on DBD stability is based on PDB 2RMN. Of note, TP63 DBD has a high overall stability ($\Delta G \sim$ 10 kcal/mol) as compared with TP53 DBD (Klein et al., 2001). Hence, the predicted stability changes will most likely not lead to complete unfolding as known for TP53 DBD mutations, but only to local structural changes that might modify DNA binding.

Abbreviations: DBD, DNA-binding domain; PDB, protein data bank.

[1]These tools predict a destabilizing mutation (as $\Delta\Delta G < 0$).

[2]These tools predict a destabilizing mutation (as $\Delta\Delta G > 0$).